Seepage into Drifts with Mechanical Degradation

Guomin Li* and Chin-Fu Tsang

Earth Sciences Division
Ernest Orlando Lawrence Berkeley National Laboratory
Berkeley, CA 94702, USA

Abstract Seepage into drifts in unsaturated tuff is an important issue for the long-term performance of the potential nuclear waste repository at Yucca Mountain, Nevada. Drifts in which waste packages will potentially be emplaced are subject to degradation in the form of rockfall from the drift ceiling induced by stress relief, seismic, or thermal effects. The objective of this study is to calculate seepage rates for various drift-degradation scenarios and for different values of percolation flux for the Topopah Spring middle nonlithophysal (Tptpmn) and the Topopah Spring lower lithophysal (Tptpll) units. Seepage calculations are conducted by (1) defining a heterogeneous permeability model on the drift scale that is consistent with field data, (2) selecting calibrated parameters associated with the Tptpmn and Tptpll units, and (3) simulating seepage on detailed degraded-drift profiles, which were obtained from a separate rock mechanics engineering analysis. The simulation results indicate (1) that the seepage threshold (i.e., the percolation flux at which seepage first occurs) is not significantly changed by drift degradation, and (2) the degradation-induced increase in seepage above the threshold is influenced more by the shape of the cavity created by rockfall than the rockfall volume.

Keywords: Unsaturated flow; Drift degradation; Seepage; Heterogeneity; Yucca Mountain, Nevada

* Corresponding author. Phone: +1-510-495-2202; Fax: +1-510-486-6115; E-mail: gmli@lbl.gov

1. INTRUDUCTION

Seepage of water into drifts in unsaturated tuff is an important issue for the long-term performance of the potential nuclear waste repository at Yucca Mountain, Nevada. The amount of water flowing into a drift controls the corrosion rates of waste packages, the waste mobilization rates, and transport rates of radionuclides leaving the drift.

Philip et al. (1989) presented the general theory of water entry into subterranean openings from steady, uniform downward flow, and developed an analytical solution to the exclusion problem for circular cylindrical cavities acting as capillary barriers. At the stagnation point at the crown of a cylindrical opening or a drift, water accumulated, reaching locally saturated conditions, and eventually seeps into the drift. Capillary forces associated with the pores in the host medium can retain the water under unsaturated conditions. The capillary pressure is reduced by the accumulation of water above the crown of the cavity, and seepage processes can occur when the capillary pressure no longer balances gravitational forces.

Tsang et al. (1997) have shown that, while seepage into a drift in an homogeneous medium occurs for a certain percolation flux, heterogeneity rises to seepage for a smaller percolation flux. This lower-seepage threshold mainly results from channelized flow in the heterogeneous fracture (Tsang and Neretnieks, 1998; Tsang et al., 2001). This is confirmed by the work of Nitao (1997), who in a 3-D modeling study of flow around a drift found that homogeneous models can underpredict seepage, because they do not account for the preferential flow paths that “weep” at relatively low percolation fluxes.

Tsang et al. (1997) and Birkholzer et al. (1999) analyzed the seepage problem using a stochastic fracture continuum model that accounts for the heterogeneity of the flow field in the fractured formation. In these papers, seepage into drifts was evaluated by first developing stochastic representations of hydrological properties and performing multiple realizations of the permeability field around the drift. Then, numerical models were used to simulate the 3-D flow of water in the fractured host rock in the vicinity of potential emplacement drifts under ambient conditions. These simulations need realistic input model parameters, which are provided by Finsterle et al. (2002), who used the code iTOUGH2 to calibrate mean parameters for the middle nonlithophysal (Tptpmn) and the lower lithophysal (Tptpll) units at Yucca Mountain.

The formation around the drifts, in which waste packages will potentially be emplaced, is subject to mechanical degradation in two ways. First, the permeability may change near the drift wall because of the excavation process and stress-release caused by the excavated cavity. Second, multiple fractures present in the rock, may form blocks that can become loose and fall into the drift. Either type of drift degradation will influence rates of seepage into drifts.

The objective of this paper is to calculate the rate of seepage into drifts for various scenarios of mechanical degradation and different values of percolation flux. Section 2 briefly describes the heterogeneous fracture continuum model. Section 3 will present property parameters and scenarios of drift degradation used in our seepage simulations. In Section 4, numerical calculations for the different scenarios and their results of seepage rate are discussed as a function of percolation fluxes. We use three realizations

of the permeability field from which the spread of results provides an indication of geostatistical variation. Finally, a discussion of technical observations and conclusions from these results is presented in Section 5.

2. THE SEEPAGE MODEL

Our conceptual model is a heterogeneous permeability field for the fracture continuum generated with parameters discussed below. The field was generated using the Sequential Indicator Simulation (SISIM) module of the Geostatistical Software Library (GSLIB) package (Deutsch and Journal, 1998). This model was described by Birkholzer et al. (1999).

Numerical simulations for seepage into drift are performed using the multicomponent, multiphase codes TOUGH2 (Pruess, 1991). However, we activate one phase and one component (i.e., liquid water) under isothermal conditions, which means Richards' equation is used for fluid flow with gas as a passive constituent. Relative permeability is related to capillary pressure and water saturation by the van Genuchten characteristic functions (van Genuchten, 1980).

According to the actual design concept of the potential waste repository, the drift is a cylinder with axes horizontal and its diameter is 5.5 m. The 3-D permeability field is 19.22 m vertical, 15.25 m wide normal to drift axis, and 10.065 m along the drift axis. The calculation mesh consists of over 100,000 grid cells, each with dimensions of 0.305 m × 0.305 m × 0.305 m.

Side boundary conditions are no-flow, the lower-boundary condition is gravity drainage, and the upper-boundary surface is simulated by an extra grid cell with a constant source

of percolation flux connected to all the grid cells in the top row. Flow is thus free to move into these extra-cells according to local conduction. Regarding the no-flow boundary condition on the two vertical planes at the end of the waste package normal to the drift axis: for a homogeneous medium, these planes are symmetrical planes between successive waste packages, and a no-flow boundary condition is justified. For a heterogeneous system, one question is the length of the flow domain versus the spatial correlation length λ of the heterogeneous medium. Based on an analysis of air-injection tests in the middle nonlithophysal (Tptpmn) and lower lithophysal (Tptpll) units at Yucca Mountain, Finsterle et al. (2002) found that data indicate the heterogeneous fields with no spatial correlation. In this case, the no-flow boundary is a reasonable approximation.

At the curved wall of the drift, the nodal distance between the drift surface and the grid cell representing the inside space of the drift is set to be very small, and thus the boundary condition can be applied directly at the drift wall. The length of the last vertical connection between the drift wall and the neighboring blocks representing the formation is set equal to 0.05 m. Our choice of this 0.05 m vertical connection to the drift wall implies a direct gravity-controlled vertical flow, with no horizontal diversion within this 0.05 m distance.

The model described above was tested for a simple case. From the analytical solution of Philip et al. (1989), we can establish whether or not water enters the drift for a given combination of percolation flux, characteristic drift length, saturated hydraulic conductivity and α', where α' is a fitting parameter controlling the rate of relative permeability decrease with increasing capillary pressure in the Gardner model (1958). A

threshold percolation flux is defined as the critical value above which water will enter the drift.

In our model, calculations were made by assigning a constant permeability of $10^{-13}m^2$ to the entire fracture continuum. Thus, a homogeneous model structure is used, with permeability of $10^{-13}m^2$ and the fitting parameter α for the van Genuchten relationship of 0.001 $1/P_a$. The van Genuchten relationship between relative permeability and capillary pressure is used in our model, whereas Philip et al. (1989) used the Gardner relationship. Birkholzer et al. (1999, Appendix A) showed that the Gardner-equation with $\alpha' = 0.0025$ can be approximated with the van Genuchten relationship with its parameter $\alpha = 0.001$ $1/P_a$. This is used in the model calculation.

In Figure 1, we present steady-state seepage rate as a function of percolation flux. The steady-state seepage rate into the drift is expressed as a fraction of the inflow into the model area over a 5.5 m width of the upper boundary (i.e., over the width or diameter of the drift). The relative seepage rate, calculated from the numerical model, steadily increases with the percolation rate from a threshold value. A threshold percolation flux is defined as the critical value above which water will seep into the drift. The threshold percolation flux is calculated at 445.73 mm/yr from the analytical solution of Philip et al. (1989), but numerical results indicate that seepage begins at percolation flux 440 mm/yr. The threshold percolation flux calculated with our numerical model is very close that calculated from the analytical solution of Philip et al. (1989). Thus, the approximate agreement provides some verification of our simulation and modeling results. Further verification studies have been made by Houseworth et al. (this issue)

3. INPUT PARAMETER SETS

The US Department of Energy is investing the feasibility of using the unsaturated zone at Yucca Mountain, NV, as a permanent storage facility for the disposal of high-level nuclear waste (Bodvarsson et al., 1999).

Fracture continuum permeability k_{FC}, van Genuchten $1/\alpha$ value, and standard deviation σ of $\ln(k_{FC})$ are the most important parameters affecting drift seepage. Standard deviation is a measure of permeability-field heterogeneity (Birkholzer et al., 1999).

Air-injection testing is a standard method to obtain drift-scale fracture-permeability values (Wang et al., 1999) and these estimates are used to condition the generation of a random permeability field. Excavation has been shown to increase the permeability around the niches excavated in the Exploratory Studies Facility (ESF) at Yucca Mountain (Wang et al., 1999; Wang and Elsworth, 1999). Since seepage is determined by the formation properties within the boundary layer in the immediate vicinity of the opening, it is reasonable to use post-excavation air-permeability data for seepage calculations.

For the van Genuchten $1/\alpha$ value, Finsterle et al. (2000) analyzed *in-situ* seepage data and provided a calibrated mean of 871 Pa for the lower lithophysal unit (Tptpll), with the interval from 740 to 1020 Pa containing 2/3 of the $1/\alpha$ values from their multiple realization studies. For the middle nonlithophysal unit (Tptpmn), Finsterle et al. (2000) provided a calibrated mean for log $(1/\alpha)$ of 2.77 and standard deviation of 0.5, which translates to a mean for $1/\alpha$ of 589 Pa and the values at one standard deviation above and below the mean for $1/\alpha$ of 525 Pa to 660 Pa, respectively.

For three niches in the middle nonlithophysal zone, Finsterle et al. (2000, Table 4) gives values for the standard deviation of fracture continuum permeability in log base 10 varying from 0.72 to 0.84, which translates to a standard deviation σ (in nature log k_{FC}) of 1.66 to 1.93. For the lower lithophysal unit, Finsterle et al. (2000, Table 4) gives a log base 10 standard deviation of 0.21, corresponding to σ in $\ln(k_{FC})$ of 0.48. This is, however, based on six measurements in one borehole only. In a numerical study of seepage from a heterogeneous fracture continuum into a drift, Birkholzer et al. (1999) found that drift seepage tracks the probability for finding local ponding in the heterogeneous field and, further, that the ponding probability is smaller for smaller standard deviations in the permeability field. Hence, less seepage is expected for smaller σ values.

After reviewing these data, we chose three parameter sets for this study which may be representative of the Yucca Mountain site. The first set, Set A, is the set of calibrated mean parameters for the middle nonlithophysal zone given by Finsterle et al. (2000):

$$\left.\begin{aligned} k_{FC} &= 1.38\times10^{-12}\,m^2 \\ 1/\alpha &= 589Pa \\ n &= 2.55 \\ \sigma &= 1.93 \end{aligned}\right\} \quad \text{Set A (Tptpmn)}$$

where k_{FC} is the mean permeability, α and n are the van Genuchten parameters, and σ is the standard deviation of $\ln(k_{FC})$. The second parameter set, Set B, is chosen to be the set of calibrated mean parameters for the lower lithophysal unit:

$$\left.\begin{aligned} k_{FC} &= 1.86\times10^{-11}\,m^2 \\ 1/\alpha &= 871Pa \\ n &= 2.57 \\ \sigma &= 1.93 \end{aligned}\right\} \quad \text{Set B (Tptpll)}$$

Here σ=1.93 is used for both sets as a more conservative value.

Numerous lithophysal cavities were present in the lower lithophysal unit (Tptpll). Thus, to include the influence of these lithophysal cavities on the seepage calculation, an additional parameter set, Set B′, is chosen for the Tptpll unit. This parameter set is the same as that of Set B, except the $1/\alpha$ value is reduced to 537 Pa to account for the overall effects of the lithophysal cavities in the medium on seepage. As discussed by Finsterle et al. (2000) lithophysal cavities tend to increase seepage.

Four values of percolation flux Q_p are used, 14.6, 73.2, 213, and 500 mm/yr. Wu et al. (1999) calculated the percolation flux expected at the repository level, based on a 3-D unsaturated zone model of Yucca Mountain. They obtained an average fracture flux of 4 to 5 mm/yr at the repository level under present climate conditions. Ritcey and Wu (1999) found that, under a climate scenario simulating the most recent glacial period, the

percolation flux ranges from 0 to 120 mm/yr, with the peak of the probability distribution around 20 mm/yr. We choose the upper limit of 500 mm/yr to accommodate potential flow focusing in the geologic layers above the drift and to safely bracket an uncertainty range more than four times the high flux value of 120 mm/yr. For seepage model with set B and B′ in the Tptpll unit (where seepage is zero for Q_p = 500 mm/yr), even larger Q_p values, 1000, 1500, 2000, and 2500 mm/yr, are used to find when seepage might occur.

4. SEEPAGE ENHANCEMENT WITH MECHANICAL DEGRADATION

Drift degradation induced by stress relief, seismic, or thermal effects may occur in three ways: (1) loosening of rock blocks and hence wider fracture aperture (fracture dilation) (Figure 2, lower left), (2) rockfall from the drift wall (Figure 2, upper left and right) and (3) extended rock failure above the drift ceiling (Figure 2, lower right).

4.1. Fracture Dilation

Because of excavation, stress is relieved at the drift, and fractures are expected to dilate at certain areas around the drift. Such fracture dilation depends on the orientation of the fracture set and generally occurs within one drift radius (Brekke et al., 1999, pp.E3-E29). An increase in fracture aperture generally causes an increase in fracture permeability and a decrease in $1/\alpha$ value. The measured increase in permeability from the pre-excavation to the post-excavation values (Wang and Elsworth, 1999) is a result of this effect. In this sense, Parameter Set A, Set B, and Set B′, which are based on *in situ* post-excavation calibration results, already have taken this into account. This means that the rock properties already represent the total effect of the near-field disturbed zone.

The possibility exists that new fractures may be formed during stress relief. In general, an increase in k_{FC} could results either from an increase in the number of fractures or an increase in aperture. It is only in the latter case that $1/\alpha$ will decrease. Thus, that portion of k_{FC} increase resulting from the creation of new fractures will accompany by a decrease in $1/\alpha$ values. In this case, k_{FC} will increase with a relatively smaller decrease in the $1/\alpha$ value. Tsang and Li (2000) indicated that seepage is smaller for correlated k_{FC}-α assumption than that for uncorrelated case. For this reason, in our study, the uncorrelated k_{FC}-α assumption is used for conservation.

4.2. Rockfall from the Drift Wall

Kicker et al. (2000) calculated rockfall probability in the drifts, under various scenarios, based on fracture maps in the ESF at Yucca Mountain. For the middle nonlithophysal zone (Tptpmn), the number of key blocks per kilometer of the drift was calculated to be less than 44, and the volume of total rockfall per kilometer to be less than 36 m^3. This implies that rockfall occurs on the average of one block every 23 m and that the mean size of the block is about 0.8 m^3. The result also indicated that 80% of the blocks are smaller than 1 m^3 (Kicker et al., 2000). Brekke et al. (1999, pp.E3-E29 by Hart) used a 2-D discrete-element method and found rockfall to occur at the spring line of the drift, with the size of the block depending on the assumed fracture spacing. To study the effect of rockfall on seepage, we made two calculations, one in which a 1.0 m^3 block was taken out from the crown of the drift, and the second in which the 1.0 m^3 block was taken out at the spring line (Figure 2, two upper cases).

Table 1 presents the calculated seepage percentages for Set A for three stochastic realizations (R1, R2, and R3), with drift-degradation modes as defined in Figure 2 (two upper cases), and compares them with the no-degradation case. Three realizations follow identical trends and the spread of results should give an indication of the geostatistical distribution. Only the cases for percolation flux Q_p = 500 mm/yr are shown. Seepage percentage is defined as the ratio of liquid that seeped into the drift to the total liquid arriving on a cross-sectional area corresponding to the footprint of the drift. Results show that the effect of a single rockfall is not significant for seepage. Calculations were also made with Set B and B′, resulting in zero seepage for all cases, with or without drift degradation.

4.3. Extended Rock Failure at the Drift Ceiling

Over time, extended rock failure may occur at the ceiling of the drift. This is schematically represented by the lower-right part of Figure 2. In the present study, detailed degraded drift profiles calculated using a discrete, regional key-block analysis (Kicker et al., 2000) were used for seepage simulation. The key-block analysis provides the following detailed 3-D drift shapes for seepage simulations, using 0.305 m (1 foot) grid size.

For the middle nonlithophysal unit (Tptpmn):

1) The greatest degradation (largest rockfall volume) shape (Figure 3)

2) Profile at 75th percentile (explanation, see below, Figure 4)

3) Base case (no degradation, with probability of 91.9%).

For the lower lithophysal unit (Tptpll), set B':

1) The greatest degradation (largest rockfall volume) shape

2) Profile at 75th percentile (explanation, see below)

3) Base case (no degradation, with probability of 99.6%).

The 75th percentile case corresponds to a rockfall valume per unit length that is greater than the rockfall volume per unit length in 75 % of the overall emplacement drift length for that rock unit. For Tptpmn, (100%–91.9%) = 8.1% of the drift length exhibits drift degradation. Of the 8.1% that does exhibit degradation, the 75% of the 8.1% has rockfall volume less than that shown in the 75th-percentile drift profile. Similarly for Tptpll, (100%–99.6%) = 0.4% of the drift length exhibits drift degradation, with the 75th percentile profile indicating that 75% of the 0.4% of the drift length has extended rock-failure volume less than that shown.

Using these 3-D degradation profiles, simulations were made to evaluate the impact of extended rock failure on seepage. Table 2 presents the seepage percentages for Set A of the middle nonlithophysal unit with drift-degradation modes (a) greatest degradation case and (b) degradation at 75th percentile, to compare with the base case.

A series of percolation flux values were used up to 500 mm/yr to explore the effect of drift degradation on seepage threshold. The results in Table 2 show that the effect of extended rock failure for seepage threshold is small for all three realizations. This can perhaps be explained by the fact that, under vertical percolation flux in a heterogeneous medium, a factor affecting the seepage is the horizontal cross section (footprint) of the drift together with the heterogeneity structure (i.e., σ and λ). If the cross-sectional area

does not change very much, the seepage threshold will also not change very much. Figure 5 shows the calculated seepage percentage as a function of percolation flux Q_p.

The results further show that seepage enhancement caused by drift degradation ranges from 0 to 5 percentage points for the percolation flux up to 500 mm/yr for the greatest degradation case and 75th percentile case. In this case, the enhancement is not larger for the greatest degradation case than the 75th percentile case. In fact, it is the other around. Perhaps the shape of the cavity in the ceiling may be more important than the volume.

Table 3 presents the seepage percentages for Set B′ of the lower lithophysal unit with drift-degradation modes, the greatest degradation case and degradation at 75th percentile, to be compared with the base case. A series of percolation flux values were used up to 2,500 mm/yr to explore the effect of drift degradation on seepage threshold. Figure 6 shows the calculated seepage percentage as a function of percolation flux Q_p. Again, the results indicate that the seepage threshold is not significantly affected by drift degradation; the seepage enhancement is two percentage points or less.

Figures 7a, 7b and 7c illustrate the saturation profile around the drift for two degradation scenarios and the base case in the Tptpmn unit with Set A. Seepage into drifts occurs when the saturation of a grid element next to the drift boundary is close to 100%; i.e., it is fully saturated and its capillary suction drops to zero. For the base case, seepage into drift depends on details of the heterogeneity in the vicinity of the drift, which acts as a capillary barrier. Figure 7a shows local heterogeneity causes water to accumulate the ceiling of drift and enter into the drift. The drift degradation changes the geometry of the boundary condition around the drift. Figure 7b shows the greatest degradation case, with

some water seeping into the drift. Some water also flows around drift and then seeps into the drift as well. For the 75th percentile case, in Figure 7c, the extended rock failure acts as local blockage on the left hand side of the drift ceiling that causes water to accumulate at the ceiling and enter the drift.

The drift provides a partial barrier to downward percolation flux in the region immediately below it. For the case in which the water seeping into the drift is removed through an engineered drainage system, directly below the drift will be a dryer, "shadow" zone. This dryer zone will decrease in width with depth below the drift. The vertical extent of the shadow zone depends on both k_{FC} and $1/\alpha$ values (Philip et al. 1989). Figures 7a-c also show the saturation profiles up to one drift diameter below the drift for Set A, with Q_p=500 mm/yr for degradation and no-degradation scenarios. The figures show that the effect of drift degradation on the shadow zone is not significant. More detail study on the shadow zone is provided by Houseworth et al. (2000, this issue).

Calculations were also made with Set B, resulting in zero seepage for all cases with percolation flux up to 2,500 mm/yr, with or without drift degradation.

5. SUMMARY AND CONCLUSIONS

A 3-D heterogeneous numerical model was developed and used to study steady-state flow around a drift for a variety of permeability fields and rock parameters. Our numerical model was verified against the analytical solution of Philip et al. (1989) by assigning a constant fracture permeability for the entire fracture continuum. The simulation results show good agreement between the two models used for calculating the threshold percolation flux.

Both rockfall and extended rock-failure effects have been analyzed by simulation. To study the effect of rockfall on seepage, we developed two scenarios, one in which a 1.0 m^3 block was taken out from the crown of the drift, and one in which the 1.0 m^3 block was taken out at the spring line. For the extended rock-failure case, the model was built by the use of detailed drift profiles from a 3-D key-block analysis, and by incorporation of calibrated mean parameters for the Tptpmn and the Tptpll units (Kicker et al., 2000).

Simulation results (Tables 1-3) show the impact of various factors on seepage. The spread of results from three realizations gives an indication of geostatistical variation. These results show that for both the Tptpmn and Tptpll units, simulated seepage enhancement caused by mechanical degradation is calculated to be small for the rockfall scenarios and relatively larger for the extended rock-failure scenarios. These seepage enhancements are large for larger percolation flux (Q_p) values. For the extended failure scenarios, seepage enhancement is between 0 and 5 percentage points for the Tptpmn unit in all three realizations, and less than 2 percentage points for the Tptpll. The enhancement does not seem to be dependent on whether it is the greatest degradation case (i.e., largest extended rock failure) or 75th percentile. Seepage threshold, on the other hand, was unaffected in almost all cases.

ACKNOWLEDGMENTS

Review and comments by Stefan Finsterle, Sumit Mukhopadhyay and Daniel Hawkes are much appreciated. This work was supported by the Director, Office of Civilian Radioactive Waste Management, U.S. Department of Energy, through Memorandum Purchase Order EA9013MC5X between Bechtel SAIC Company, LLC and the Ernest

Orlando Lawrence Berkeley National Laboratory (Berkeley Lab), under the auspices of U.S. Department of Energy Contract No. DE-AC03-76SF00098.

REFERENCES

Birkholzer, J.T., Li, G., Tsang, C.-F., and Tsang, Y., 1999. Modeling studies and analysis of seepage into drifts at Yucca Mountain. J. Contaminant Hydrol., 38, (1–3): 349–384.

Bodvarsson, G.S., Boyle, W., Patterson, and Williams, D., 1999, Overview of scientific investigations at Yucca Mountain – The potential repository for high-level nuclear waste. J. Contaminant Hydrol., 38, (1–3): 3–24.

Brekke, T.L., Cording, E.J., Daemen, J., Hart, R.D., Hudson, J.A., Kaiser, P.K., and Pelizza, S., 1999. Panel report on the Drift Stability Workshop. Drift Stability Workshop, Las Vegas, Nevada, December 9–11, 1998. Las Vegas, Nevada.

Deutsch, C.V. and Journal, A.G., 1998. GSLIB-Geostatistical Software Library and User's Guide (Second Edition), Oxford Univ. Press, New York.

Finsterle, S., C. F. Ahlers, R. C. Trautz, and P. J. Cook, Inverse and predictive modeling of seepage into underground openings, Journal of Contaminant Hydrology, this issue.

Finsterle, S., Ahlers, C.F., and Trautz, R.C., 2000. Seepage Calibration Model and Seepage Testing Data, MDL-NBS-HS-000004 REV01. Civilian Radioactive Waste Management System Management and Operating Contractor (CRWMS M&O): Las Vegas, Nevada. (Lawrence Berkeley National Laboratory: Berkeley, California.)

Gardner, W.R., 1958. Some steady state solutions of the unsaturated moisture flow equation with application to the evaporation from a water table. Soil Sci., 85: 288–322.

Houseworth, J.E., Finsterle, S., and Bodvarsson, G.S., 2002. Radionuclide transport in the drift shadow. J. Contaminant Hydrol., this issue.

Li, G. and Tsang, C.-F., 2000. Seepage Model for PA Including Drift Collapse. MDL-NBS-HS-000002 REV01. CRWMS M&O, Las Vegas, Nevada.

Kicker, D.C., Lin, M., and Kemeny, J., 2000. Drift Degradation Analysis. ANL-EBS-MD-000027 REV 01. CRWMS M&O, Las Vegas, Nevada.

Nitao, J.S., 1997. Preliminary bounds for the drift-scale distribution of percolation and seepage at the repository level under pre-emplacement conditions. Yucca Mountain Project Deliverable No. SPLB1M4. Lawrence Livermore National Laboratory, Livermore, California.

Philip, J.R., Knight, J.H., and Waechter, R.T., 1989. Unsaturated seepage and subterranean holes: conspectus and exclusion problem for circular cylindrical cavities. Water Resour. Res., 25: 16–28.

Pruess, K., 1991. TOUGH2 – A general purpose numerical simulator for multiphase fluid and heat flow. Report LBL-29400, Lawrence Berkeley National Laboratory, Berkeley, California.

Tsang, C.-F., Birkholzer, J.T., Li, G., and Tsang, Y., 1997. Drift-scale modeling: Studies of seepage into a drift. Yucca Mountain Project Level 4 Milestone Report SP331DM4. Report LBNL-41046, Lawrence Berkeley National Laboratory, Berkeley, California.

Tsang, C.-F. and Neretnieks, I., 1998. Flow channeling in heterogeneous fractured rocks. Reviews of Geophysics, 36, (2): 275–298.

Tsang, C.-F. and Li, G., 2000. Seepage Model for PA Including Drift Collapse. MDL-NBS-HS-000002 REV00. CRWMS M&O, Las Vegas, Nevada.

Tsang, C.-F., Tsang, Y.W., Birkholzer, J.T., and Moreno, L., 2001. Dynamic modeling of flow and transport in saturated and unsaturated heterogeneous media. In: D.D. Evans, T.J. Nicholson and T.C. Rasmussen (Editors), Flow and Transport Through Unsaturated Fractured Rock, Geophysical Monograph Series Volume 42, Second Edition, AGU, Washington D.C. 33–44.

Ritcey, A.C. and Wu, Y.S., 1999. Evaluation of the effect of future climate change on the distribution and movement of moisture in the unsaturated zone at Yucca Mountain, Nevada. J. Contaminant Hydrol., 38, (1–3): 257–279.

Van Genuchten, M.T., 1980. A closed-form equation for predicting the hydraulic conductivity of unsaturated soil. Soil Sci. Soc. J., 44: 892–898.

Wang, J.S.Y. and Elsworth, D., 1999. Permeability changes induced by excavation in fractured tuff. Proceedings of the 37th U.S. Rock Mechanics Symposium, Rock Mechanics for Industry, 2, The American Rock Mechanics Association, Alexandria, Virginia, pp. 751–757.

Wang, J.S.Y., Trautz, R.C. Cook, P.J., Finsterle, S., James, A.L., and Birkholzer, J., 1999. Field tests and model analyses of seepage into drift. J. Contaminant Hydrol., 38, (1–3): 323–347.

Wu, Y-S., Haukwa, C., and Bodvarsson, G.S., 1999. A site-scale model for fluid and heat flow in the unsaturated zone of Yucca Mountain, Nevada. J. Contaminant Hydrol., 38, (1–3): 185–215.

Table 1. Seepage Percentage for Rockfall Scenarios, for Qp = 500 mm/yr and Set A

Condition	Seepage Percentage		
	R1	R2	R3
Base case	7.1	7.1	13
1 m rockfall from crown of drift	7.2	7.3	12
1m rockfall from springline of drift	7.1	7.1	13

Note: R1, R2, and R3 are Realization 1, Realization 2, and Realization 3, respectively.

Table 2. Seepage Percentage for Set A Extended Rock-Failure Scenarios

Q_p (mm/yr)		14.6	73.2	213.4	500
Base Case	R1	0.0	0.0	0.46	5.69
	R2	0.0	0.0	0.82	11.04

	R3	0.0	0.0	0.15	10.71
	Average	0.0	0.0	0.48	9.15
The Greatest Degradation Case	R1	0.0	0.0	0.48	8.97
	R2	0.0	0.0	0.86	13.99
	R3	0.0	0.0	0.34	12.58
	Average	0.0	0.0	0.56	11.85
75 Percentile Case	R1	0.0	0.0	2.87	10.63
	R2	0.0	0.0	3.39	17.53
	R3	0.0	0.0	2.36	16.50
	Average	0.0	0.0	2.87	14.89

Note: R1, R2, and R3 are Realization 1, Realization 2, and Realization 3, respectively.

Table 3. Seepage Percentage for Set B' Extended Rock-Failure Scenarios

Q_p (mm/yr)		500	1000	1500	2000	2500
Base Case	R1	0.0	0.0	0.33	0.55	0.83
	R2	0.0	0.0	0.50	1.05	2.09
	R3	0.0	0.0	0.0012	1.03	2.86
	Average	0.0	0.0	0.28	0.88	1.93
The Greatest Degradation Case	R1	0.0	0.2	0.65	1.42	2.41
	R2	0.0	0.0	1.50	3.04	4.56
	R3	0.0	0.0	0.11	1.94	4.25
	Average	0.0	0.07	0.75	2.13	3.74
75 Percentile Case	R1	0.0	0.0	0.33	0.59	1.24
	R2	0.0	0.0	0.50	1.06	2.32
	R3	0.0	0.0	0.33	1.36	3.10
	Average	0.0	0.0	0.39	1.00	2.22

Note: R1, R2, and R3 are Realization 1, Realization 2, and Realization 3, respectively.

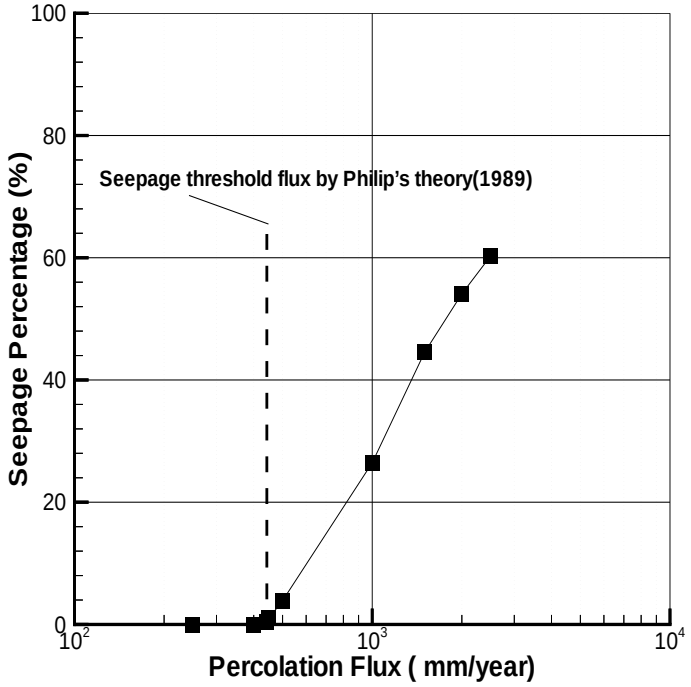

Figure 1. Seepage percentage as a function of percolation flux in the homogeneous model.

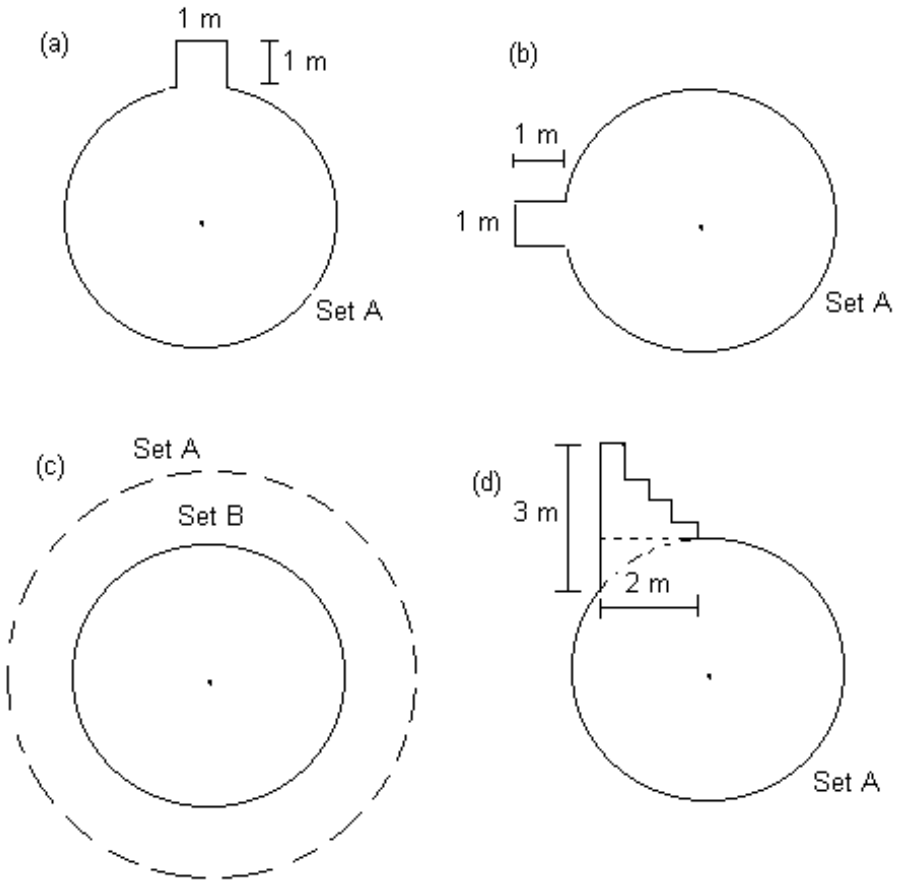

Figure 2. Drift-degradation submodel scenarios (1) fracture dilation (lower left), (2) rockfall from the drift ceiling (upper left) and from the springline (upper right), and (3) extended rock failure (lower right) (from Li and Tsang, 2000).

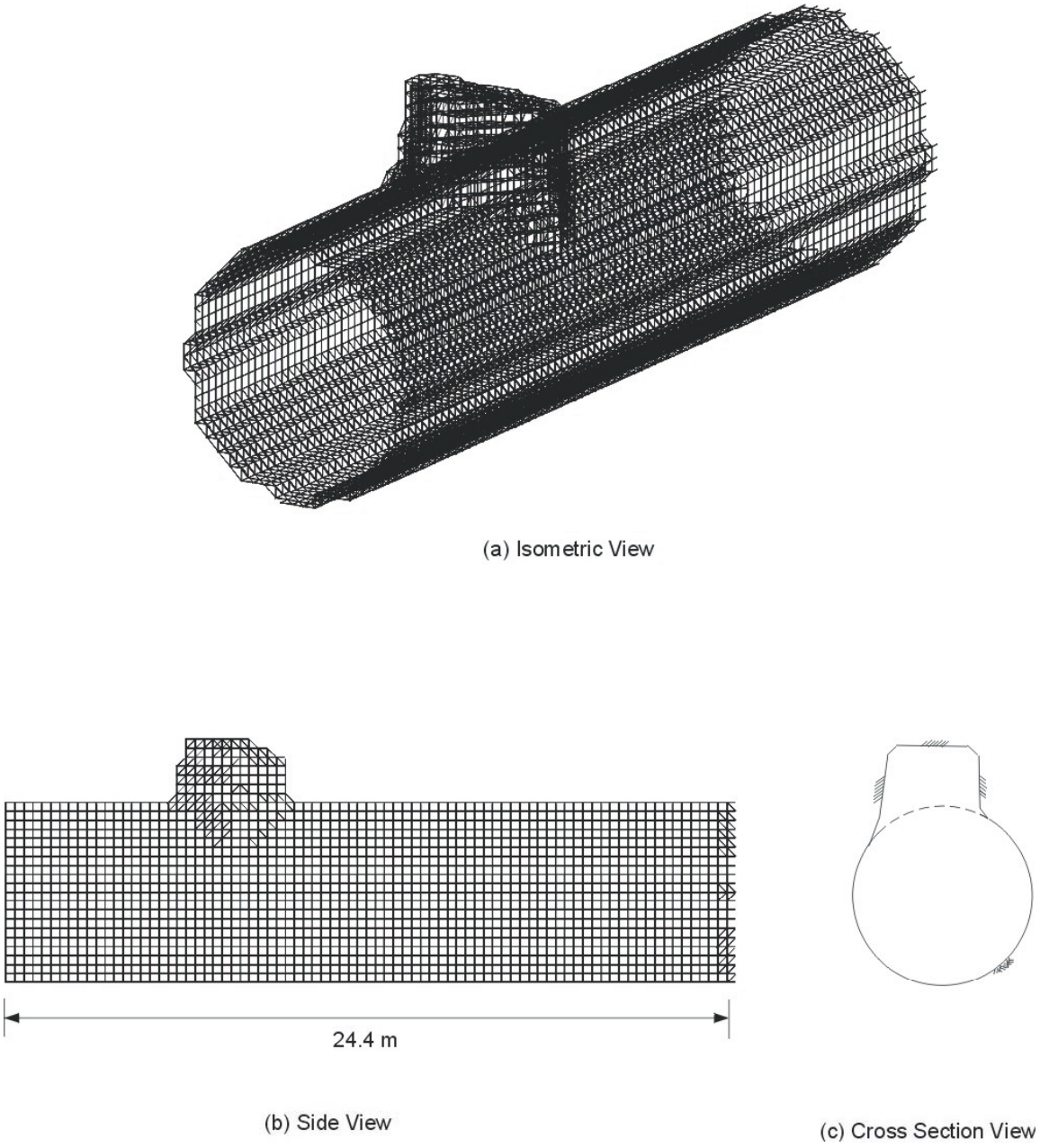

Figure 3. Emplacement drift shape for the Tptpmn Unit, the greatest degradation (provided by Kicker et al. Based on their input, Kicker et al., 2000).

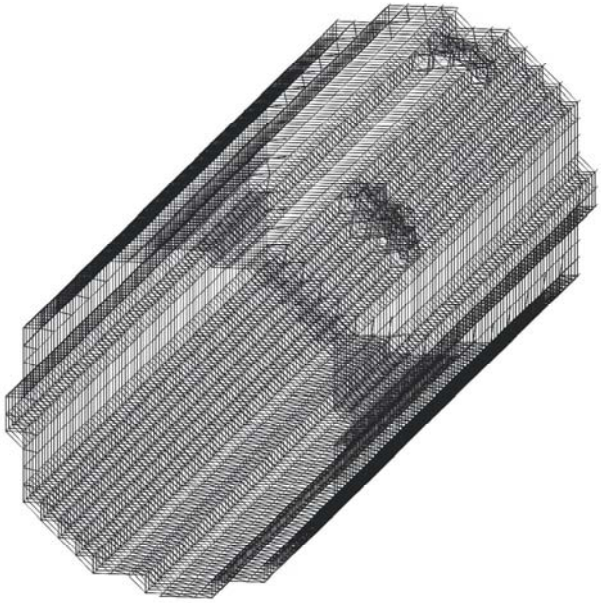

(a) Isometric View

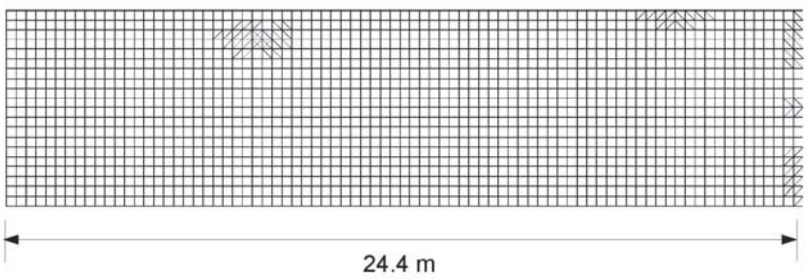

(b) Side View

(c) Cross Section View

Figure 4. Emplacement Drift Profile for the Tptpmn Unit, 75 Percentile Case(provided by Kicker et al. Based on their input, Kicker et al., 2000)

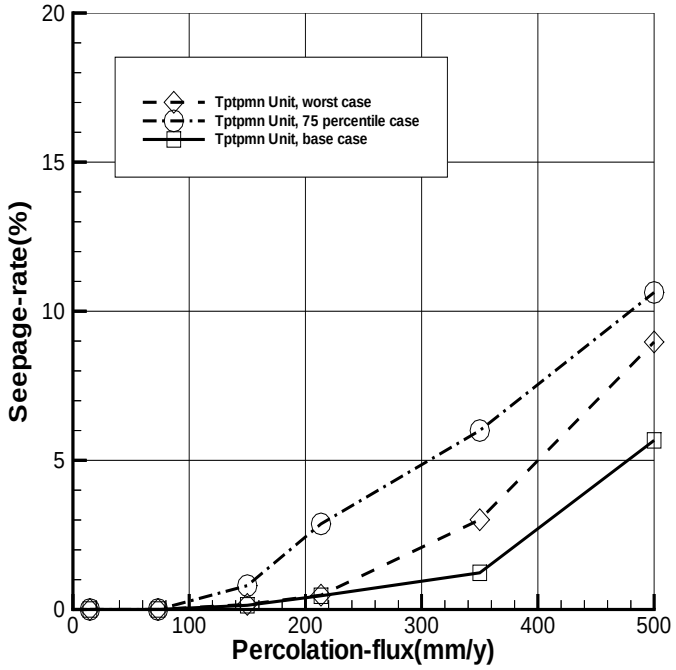

Figure 5. Seepage percentage as a function of percolation flux Q_P for the two degradation scenarios for Set A, Realization 1.

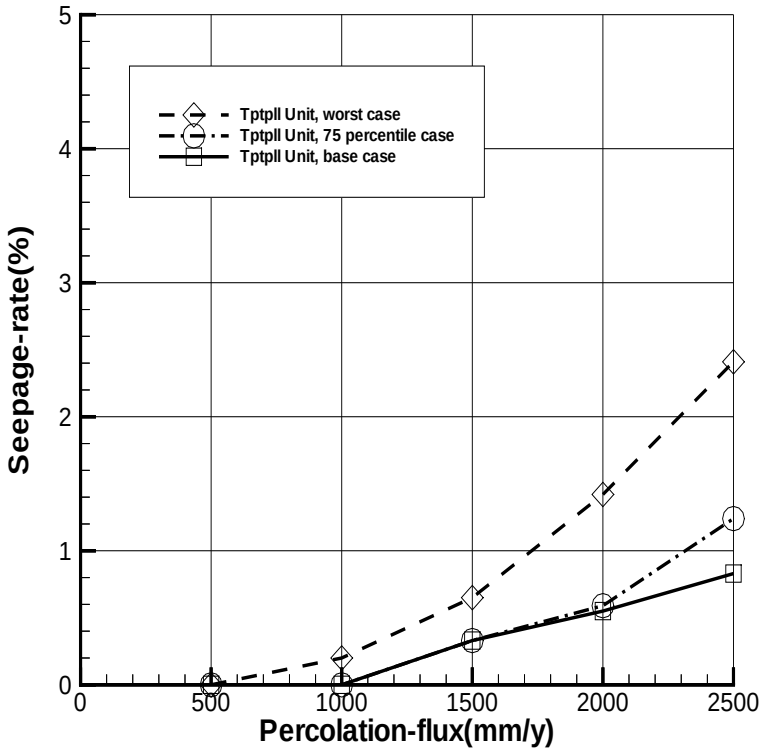

Figure 6. Seepage percentage as a function of percolation flux Q_P for the two degradation scenarios for Set B', Realization 1

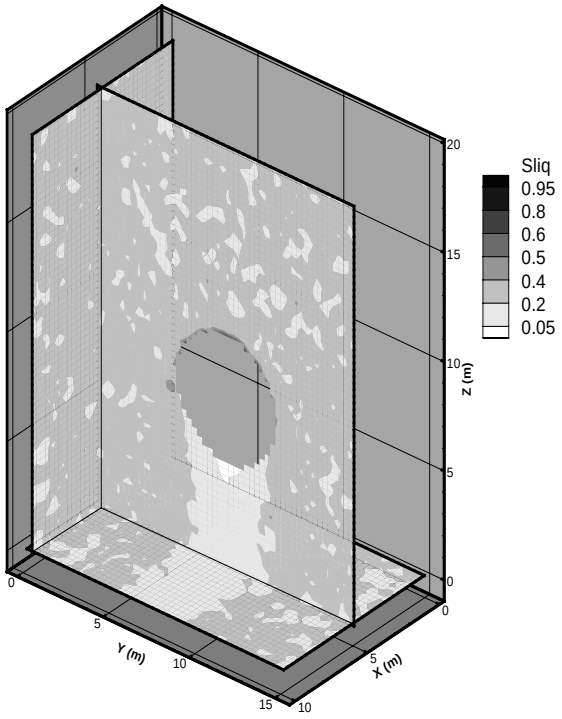

Figure 7a. Liquid saturation distribution around a drift for the base case in the Tptpmn with Set A, Realization 1

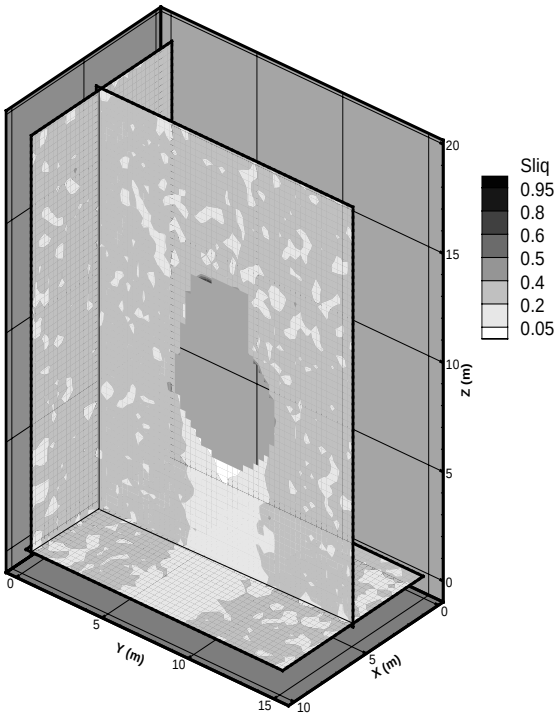

Figure 7b. Liquid saturation distribution around a drift for the greatest degradation case in the Tptpmn with Set A, Realization 1

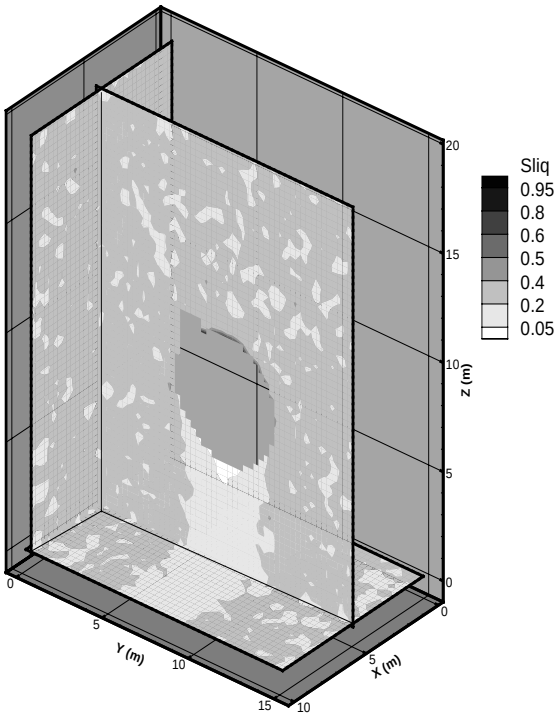

Figure 7c Liquid saturation distribution around a drift for the 75 percentile case in the Tptpmn with Set A, Realization 1.